

Synthesis and Characterization of a Novel Sm⁺³ Activated NaCdVO₄ Phosphors for Red Emitting Material

Marwa Enneffati (✉ marwa.enneffati@gmail.com)

Universite de Sfax Faculte des Sciences de Sfax <https://orcid.org/0000-0002-6607-5043>

Mohammed Rasheed

Middle Technical University Institute of Technology - Baghdad

Narjes Aouani

Taif University College of Science

Bassem Louati

University of Sfax Preparatory Engineering Institute of Sfax: Universite de Sfax Institut Preparatoire aux Etudes d'Engenieur de Sfax

Kamel Guidara

Universite de Sfax Faculte des Sciences de Sfax

Regis Barillé

University of Angers Faculty of Science: Universite Angers Faculte des sciences

Research Article

Keywords: Luminescence, phosphors, Samarium, vanadates, w-LEDs, CIE

Posted Date: July 6th, 2021

DOI: <https://doi.org/10.21203/rs.3.rs-478437/v1>

License: © ⓘ This work is licensed under a Creative Commons Attribution 4.0 International License.

[Read Full License](#)

Synthesis and characterization of a novel Sm⁺³ activated NaCdVO₄ phosphors for red emitting material

Marwa Enneffati^a, Mohammed Rasheed^{c,d}, Narjes Aouani^a, Bassem Louati^b, Kamel Guidara^b, Régis Barillé^c

^aDepartment of physics, College of Science, Taif University, Saudi Arabia

^bLaboratory of spectroscopic characterization and optic materials, University of Sfax, Faculty of Sciences
B.P. 1171, 3000, Sfax-Tunisia

^cMOLTECH-Anjou, photonics Laboratory, Angers University, 2 Bd. Lavoisier, 49045 Angers, France

^dMaterial Science, Applied Sciences Department, University of Technology, Baghdad, Iraq

Abstract

Sm³⁺ activated NaCdVO₄ phosphors were prepared by the simple solid-state reaction method. X-ray diffraction, dispersive energy (EDS), scanning electron microscope (SEM), infrared as well as photoluminescence (PL) techniques were used to characterize obtained samples. Irregular and non-uniform structures were observed by SEM. EDS spectra confirmed the presence of Na, Cd, V, O and Sm elements in each sample. Under 405nm excitation, the NaCd_{1-x}VO₄: xSm (x=0.01, 0.03 and 0.05) exhibits a bright red emission consisting mainly of four wavelength peaks at 556, 593, 650 and 700 nm. The highest emission intensity was found with a composition of x=0.05. The analysis of PL spectra suggest that studied samples can be used as a red emitting phosphors candidates for fabrication of white LEDs. The CIE chromaticity coordinates of prepared samples were close to the blue-emitting phosphors for NaCdVO₄ and red-emitting ones for NaCd_{0.99}Sm_{0.01}VO₄, NaCd_{0.97}Sm_{0.03}VO₄, and NaCd_{0.95}Sm_{0.05}VO₄. The band gap energies of phosphors were calculated from reflectance data using K-M function.

Keywords: Luminescence, phosphors, Samarium, vanadates, w-LEDs, CIE

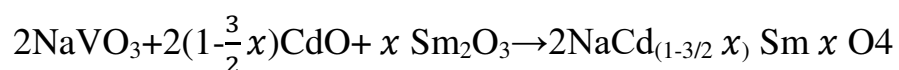
1. Introduction

In recent years, phosphors-transformed LEDs present the most promising solid-state light source compared to conventional incandescent and fluorescent lamps due to their long lifetime, high luminescence efficiency as well as environmental friendly characteristics [1-5]. Vanadate compounds containing $[\text{VO}_4]^{3-}$ present a significant family of luminophores. They show wide and intense charge transfer absorption bands in the UV region and visible emission bands in the 400-700nm region due to the $\text{O}^{2-} - \text{V}^{5+}$ charge transfer transition [6-10]. Moreover, the energy transfers from $[\text{VO}_4]^{3-}$ groups to the dopants Sm^{3+} ion through $\text{O}^{2-} - \text{V}^{5+}$ charge transfer [11]. Therefore, intense luminescence characteristics are expected in rare earth ion activated vanadates. Sm^{3+} as an important member of RE ions is an excellent activator to generate red-orange or red emissions due to intrinsic 4f-4f transitions [12-14]. Nevertheless, much effort still should be dedicated to RE ion activated vanadates to further improve their luminescence properties.

In present work, we chose as a luminescent host, the NaCdVO_4 which has a space group of Cmcm and a lattice parameter varying with concentration Sm^{3+} . Sm^{3+} -activated NaCdVO_4 phosphors were successfully prepared by conventional solid-solid technique. The structure is determined by X-ray (XRD) and confirmed by FTIR and EDX. The morphology is by SEM. Photoluminescence (PL) allow us to found the optimal concentration of dopant corresponding to the maximum of emission in visible region. The package CIE give us the chromaticity coordinates and diffusive reflectance is used in order to obtain the energy gap.

1. Experimental method

The powdered samples with general chemical formula $\text{NaCd}_{(1-3/2x)}\text{Sm}_x\text{VO}_4$ ($x=0.01, 0.03, 0.05$) were successfully synthesized via a typical solid state reaction method at high temperature of 873K according the following chemical path:



The precursor materials are NaVO_3 , CdO , and Sm_2O_3 of high purity. These materials are mixed in stoichiometric amounts in the first step. The obtained powders are pressed into pellets.

The pellets are annealed at a temperature of 873K for 12h and cooled down to the room temperature.

2. Samples characterization:

X-ray powder diffraction was used in order to check of the phases purity of prepared compounds using X'Pert PROMPD diffractometer equipped with $\text{Cu-K}\alpha$ radiation ($\lambda_{\text{Cu}}=1.5046 \text{ \AA}$). The intensity data was recorded by continuous scan in $2\theta/\theta$ mode from 10 to 60° with a step $\Delta(2\theta) = 0.017^\circ$.

The elemental composition of samples was carried out by analyzing the energy dispersive with an X-ray detector attached to the Zeiss-SEM instrument and the average size of grains was estimated.

The Infrared spectra was recorded at room temperature with a Perkin Elmer spectrophotometer in the wave number range $50\text{-}1100\text{cm}^{-1}$. The PL spectra were measured by Leica spectrophotometer equipped with a Xe lamp as excitation source.

UV-Vis spectra of investigated compounds were carried out at room temperature using UV- 3101PC scanning spectrophotometer (Integrated Sphere) in the range of wavelength (200- 800) nm.

3. Results and discussions

a. X-ray analysis

The XRD patterns of NaCdVO₄ doped Sm³⁺ ions are shown in Figure1. The obtained patterns were in close agreement with the orthorhombic structure belonging to space group Cmcm. XRD profiles of all specimens match well with our previous work [15]

It was observed that Sm³⁺ doping NaCdVO₄ did not influence the main structure of the host because no significant shift of observed peaks in series of doped samples since the doping with Sm³⁺ which it's ionic radii $r(\text{Sm}^{3+}, \text{CN}=6)=1.09 \text{ \AA}$ [16] into the Cd²⁺ ($[r(\text{Cd}^{2+}, \text{CN}=6)=0.95 \text{ \AA}]$) site is assumed owing to the small radius percentage difference Dr of both ions. In fact, the percentage difference in ionic radii between substituted and doped ions should be less than 30%.

the equation below can calculate the difference between Cd²⁺ and the doped rare ions (Sm³⁺) in radius percentage

$$Dr = 100 \times \frac{R_m(\text{CN}) - R_d(\text{CN})}{R_m(\text{CN})}$$

where Dr is the radius percentage difference; CN is the coordination number; R_m(CN) is the radius of the host cation; and R_d(CN) is the radius of the doped ion. The calculated value of Dr is about 14%.

The unit cell parameter for each sample has been refined by the least square method from

powder data and summarized in the table 1.

b. EDS and SE

In order to check of the elemental composition, a chemical analysis was performed on the different samples. Figure2 (a, b and c) shows the EDS spectra of Sm doped NaCdVO₄ (1%, 3%, and 5%). It confirms firstly that synthesized compounds have elements of Na, Cd, V, and O and the presence of samarium on the all spectra of EDS. The EDS and XRD results indicate our success of preparation of NaCd_(1-3/2x) Sm_xVO₄ (x=0.01, 0.03, 0.05) samples.

Figure3 (a, b and c) shows the size distribution histograms of NaCdVO₄: Sm (1%, 3%, and 5%) micro particles. The SEM images are also shown in Figure3 inset. The grain sizes of samples average around 1-8 μm indicating success of micro-particles synthesis.

c. Infrared spectra

The IR spectra of all investigated samples recorded at room temperature in the wavenumber range from 500 cm^{-1} to 1200 cm^{-1} are shown in Figure 4. A tentative assignment based on similar orthovanadate compounds shows that all of observed bands are assigned to the internal modes of VO_4 group. The bands observed between 500 cm^{-1} and 600 cm^{-1} in all spectra are connected to the symmetrical modes (VO_4). The anti-symmetrical stretching modes $\nu_{\text{as}}(\text{VO}_4)$ are detected in the wave number region from 600 cm^{-1} to 800 cm^{-1} while the symmetrical elongation modes $\nu_{\text{s}}(\text{VO}_4)$ are situated between 800 cm^{-1} and 1000 cm^{-1} [17-19].

The analysis of the IR spectra shows the formation of a unique phase with a good agreement with XRD results.

d. Luminescence properties

The PL emission spectra of $\text{NaCdVO}_4:\text{Sm}^{3+}$ phosphor obtained under 405 nm excitation is done in Figure 5. The emission band observed around 474 nm is due to the dominating charge transfer of $[\text{VO}_4]^{3-}$ group [20]. It is also observed that each emission spectrum of different concentration exhibits four emission bands in the visible region around 556 nm , 593 nm , 650 nm and another small peak around 700 nm which are ascribed to the electronic transitions of Sm^{3+} from the excited state $^4\text{G}_{5/2}$ to the lower energy levels $^6\text{H}_{5/2}$, $^6\text{H}_{7/2}$, $^6\text{H}_{9/2}$, and $^6\text{H}_{11/2}$ respectively [21].

The green ${}^4G_{5/2} \rightarrow {}^6H_{5/2}$ (556nm) allowed transition is purely magnetic dipole (MD) and its intensity is influenced by the environment around the Sm^{3+} ions in the host lattices, while ${}^4G_{5/2} \rightarrow {}^6H_{9/2}$ (640nm) allowed transition is purely electric dipole (ED). The strongest peak at 593 nm (${}^4G_{5/2} \rightarrow {}^6H_{7/2}$) is symmetry sensitive transition implicating that Sm^{3+} ions occupies simultaneously symmetry sites of the $NaCdVO_4$ host lattice. In addition, the shape and intensity of this peak indicate that Sm^{3+} is an excellent candidate for $NaCdVO_4$ doping under 405nm excitation wavelength.

In order to better explain the luminescence mechanism of Sm^{3+} in the $NaCdVO_4$ host, a simplify energy level diagram based on selection rules is displayed in Figure 6. The Sm^{3+} ions are firstly excited under 405nm after that due to the fast transition the ${}^4G_{5/2}$ level is populated. Then, the emissions of Sm^{3+} ion will be achieved because of the following radiative transitions, ${}^4G_{5/2} \rightarrow {}^6H_{5/2}$ at 546nm, ${}^4G_{5/2} \rightarrow {}^6H_{7/2}$ at 593nm, ${}^4G_{5/2} \rightarrow {}^6H_{9/2}$ at 640nm and ${}^4G_{5/2} \rightarrow {}^6H_{9/2}$ at 700nm.

The luminescence emission intensity of Rare earth ion-activated phosphors can be in general affected by the dopant concentration. As described in figure 5, all the samples exhibit the same characteristics of Sm^{3+} emissions as the PL profiles except the intensity. In fact, the emission intensity increased with the increase in concentration and reached a quenching concentration at $x=0.05$. This concentration is mainly due, according to the Van Uitert, to two different types of mechanism, namely exchange and electric multipole-multipole interactions [22]. The interaction mechanism can be identified through analyzing the critical distance between samarium and samarium ions.

The critical distance defined by using the following formula of Blasse's [23]:

$$R_c = 2 \left(\frac{3V}{4\pi X_c Z} \right)^{\frac{1}{3}}$$

Where R_c is the critical distance of Sm concentration, V is the volume of the unit cell, Z is and X_c is the number of cations.

For $\text{NaCd}_{0.95}\text{Sm}_{0.05}\text{VO}_4$, $V=374.174\text{\AA}^3$, $X_c=0.05$, and $Z=4$. The R_c was determined to be 15.28\AA which is larger than 5\AA . Thus, the concentration quenching mechanism for Sm^{3+} in the $\text{NaCdVO}_4:x\text{Sm}^{3+}$ is dominated by multipole-multipole interaction.

On the basis of Dexter's energy transfer expression for multipole interaction, the relation between emission intensity and activator concentration can be achieved, as defined below [24, 25]:

$$\frac{1}{X} = K \left[1 + \beta(x)^{Q/3} \right]^{-1}$$

where I present the PL emission intensity, x is the doping concentration, k and β are constants for a given host lattice and the value of Q equals to 6, 8 and 10 corresponding to dipole-dipole, dipole-quadrupole and quadrupole-quadrupole interactions, respectively. As a result of the fitting of experimental data of the plot of $\ln(I/x)$ versus $\ln(x)$ (Figure 7), the Q value was found to be 6.54. This result suggest that the energy transfer mechanism for the concentration quenching in $\text{NaCdVO}_4:\text{Sm}^{3+}$ was dipole-dipole interaction.

The CIE chromaticity coordinates are important for the performance of phosphors and have been calculated to estimate the luminous color of the phosphor material. CIE is the standard reference for defining colors and is obtained by considering the sensitivity of the human eye to different colors.

Figure 8 shows the CIE chromaticity diagram calculated from photoluminescence data. All the chromaticity (X, Y) coordinates of the prepared NaCd_{1-x}VO₄: Sm³⁺ phosphors with x= 0.01, 0.03 and 0.05 are located in the red region (X=0.33, Y=0.36), (X=0.47, Y=0.51), (X=0.43, Y=0.54), and (X=0.48, Y=0.50), respectively. This result indicates the excellent stability of NaSrVO₄: Sm phosphor which will not vary with different concentrations of Sm³⁺ ions. Therefore, the red emission phosphor is needed for high color rendering in W-LEDs.

In the order to determine the band gap, diffuse reflectance spectra were converted using the Kubelka-Munk function expressed by [26]:

$$F(R) = \frac{(1 - R)^2}{2Rt} \approx \alpha$$

Where F(R) is the Kubelka-Munk function and t (mm) is the thickness of pellets.

The energy band gap E_g of material is related to the absorption coefficient α by the following Tauc equation as [26]:

$$\alpha h\nu = B(h\nu - E_g)^m$$

Where m is equals to 2 for an indirect transition and 1/2 for a direct transition. A Tauc plots were plotted between (αhν)², (αhν)^{1/2} and hν for each sample. The shapes of these curves favor the direct transition for all compositions. The value of direct band gap E_g was obtained from the extrapolating of the linear fitted region at (αhν)=0 in the plot of (αhν)² versus hν as shown in Figure 9. The band gap energy showing an increase with of the increase of doping concentration from 3.57eV for NaCd_{0.99}Sm_{0.01}VO₄ to 3.69eV for NaCd_{0.97}Sm_{0.03}VO₄ then decreasing to 3.5eV for NaCd_{0.95}Sm_{0.05}VO₄.

4. Conclusions

Sm³⁺ doped NaCdVO₄ phosphors doped with varying concentration were prepared by a simple solid-state reaction technique. The samples were found to crystallize in the

orthorhombic system with Cmc₂m space group. The EDS spectra confirmed the presence of Sm³⁺ in all compositions. The average particle sizes were estimated in the region of 1-8 μm.

Upon 405nm excitation, the characteristic Sm³⁺-activated NaCdVO₄ were observed and the Intensity showed a maximum of emission when Sm³⁺ ion content was above 5%. It was found that the concentration quenching mechanism occurred as a result of dipole-dipole interaction according to Dexter's theory. The CIE chromaticity coordinates of the obtained phosphors suggest that can be used as red-emitting phosphor for white LEDs applications.

References

- [1] E.F. Schubert, J.K. Kim, *Science* 308 (2005) 1274.
- [2] S. Neeraj, N. Kijima, A.K. Cheetham, *Chem. Phys. Lett.* 387 (2004) 2.
- [3] J.S. Kim, P.E. Jeon, J.C. Choi, H.L. Park, S.I. Mho, G.C. Kim, *Appl. Phys. Lett.* 84 (2004) 2931.
- [4] H. Lin, W. Changand, S. Chu, *J. Lumin.* 133 (2013) 194
- [5] J. Zhao, Guo C, Yu, R.Yu, *Opt. Laser Technol.* 45 (2013) 62.
- [6] M. Ya. Khodos, B. V. Shul'gin, F.F. Gavrilov, A. A. Fotiev, and V. M Lioznyanskii, *Zhurnal Prikladnoi Spektroskopii* 16 (1972) 1023-1028.
- [7] B.V. Shul'gin, N. I. Kordyukov, F. F. Gavrilov, A. A. Fotiev, and V. Yu. Kara-Ushanov, *Russian Physics Journal* 15 (1972) 1584-1587.
- [8] R.C. Ropp, *Journal of the Electrochemical Society* 115 (1968) 940-945.
- [9] A.S. Moskvina, M. Ya. Khodos, and B. V. Shul'gin, *Zhurnal Prikladnoj Spektroskopii* 18, (1973) 54-58.
- [10] V. Yu. Kara-Ushanov, B.V. Shul'gin, A. A. Fotiev, F. F. Gavrilov, G. G. Smirnov, *Izv.Akad. NaukSSSR, Ser. Fiz.* 38 (1974)1210.
- [11] J. Wu, S. Shi, X. Wang, J. Li, R. Zong, W. Chen, *J. Mater. Chem.* 2 (2014) 2786.
- [12] R. Cao, K. Chen, P. Liu, C. Cao, Y. Xu, H. Ao, P. Tang, *Luminescence.* 30 (2015) 962.
- [13] Z. Zhang, C. Li, C. Han, J. Li, Y. Jia, D. Wang, *J. Alloys Compd.* 654 (2016) 146.
- [14] P. Biswas, V. Kumar, G. Agarwal, O.M.N twaeaborwa, H.C. Swart, *Ceramics International* 42(2016) 2317.
- [15] M. Enneffati, , B. Louati, K. Guidara, , *Ionics* 23 (2017) 1115.
- [16] Y. Q. Jia, "Crystal radii and effective ionic radii of the rare earth ions," *J. Solid State Chem.*, vol. 95, no. 1, pp. 184–187, 1991, doi: 10.1016/0022-4596(91)90388-X.
- [17] R.L. Frost, P.A. Williams, J.T. Kloprogge, P. Leverett, *Raman Spectroscopy* 32 (2001) 906-911.
- [18] J.B. Liu, H.Wang, S.Wang, H.Yan, *Materials Science and Engineering B* 104 (2003) 36- 39.
- [19] R.L. Frost, D. A. Henry, M. L. Weier, W. Martens, *Journal of Raman Spectroscopy* 37 (2006) 722-732.
- [20] T. Hasegawa, Y. Abe, A. Koizumi, T. Ueda, K. Toda, M. Sato. *Inorg. Chem.* 57 (2018) 857.
- [21] G.H. Dieke, H.M. Crosswhite, *Appl. Opt.* 2 (1963) 675.

[22] L. G. Vanuitert, *J. Lumin.* 29 (1984) 1.

[23] G. Blasse, *Phys. Lett.* 28 (1968) 444.

[24] D. L. Dexter, J. H. Schulman, *Chem. Phys.* 22 (1954) 1063.

[25] P. Du, L. K. Bharat, X. Guan, J. S. Yu, *J. Appl. Phys.* 117 (2015) 083112.

[26] M. Enneffati, N. K. Maaloul, B. Louati, K. Guidara, K. Khirouni, *Opt Quant Electron* 49 (2017) 331.

Figures captions

Figure 1: XRD patterns of NaCdVO₄:xSm phosphors

Figure 2: EDS spectra of NaCdVO₄:xSm compounds

Figure 3: Size distribution histograms of NaCdVO₄:xSm phosphors

Figure 4: IR spectra of NaCdVO₄:xSm phosphors

Figure 5: Room-temperature PL emission spectra of the as a function of wavelength under 405nm excitation

Figure 6: Schematic of the energy transfer process from [VO₄]³⁻ to Sm³⁺ in NaCdVO₄:xSm phosphors

Figure 7: Plot of log (I/x) versus log(x) for the ⁴G_{5/2}→⁶H_{7/2} transition of Sm³⁺ ions in NaCdVO₄: xSm phosphors

Figure 8: CIE chromaticity coordinates of NaCdVO₄ doped with Sm³⁺

Figure 9: Reflectance spectra of NaCdVO₄:xSm phosphors

Figure 10: Plots of (αhν)^{1/2} and (αhν)² versus (hν) of NaCdVO₄:xSm phosphors

Tables captions

Table1: Crystalline parameters of NaCdVO₄:xSm phosphor

Figures

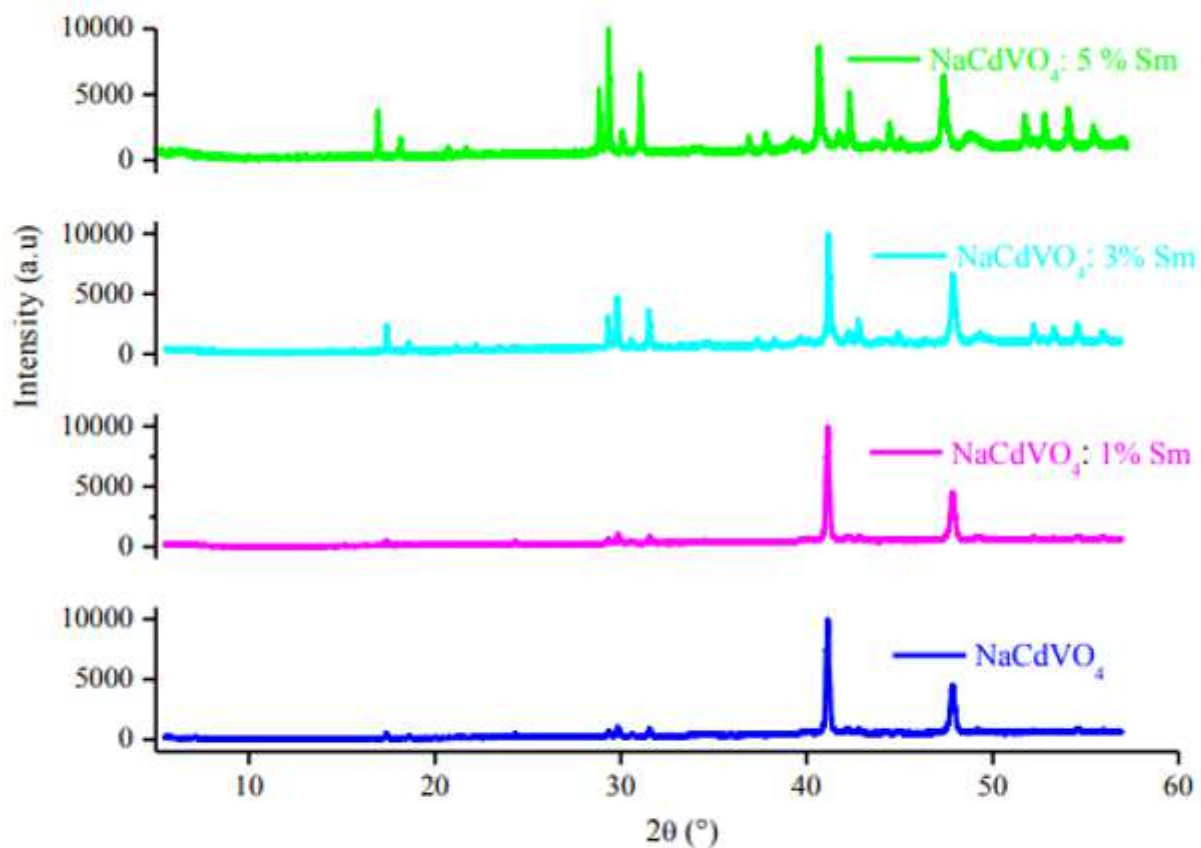


Fig.1

Figure 1

XRD patterns of NaCdVO₄:xSm phosphors

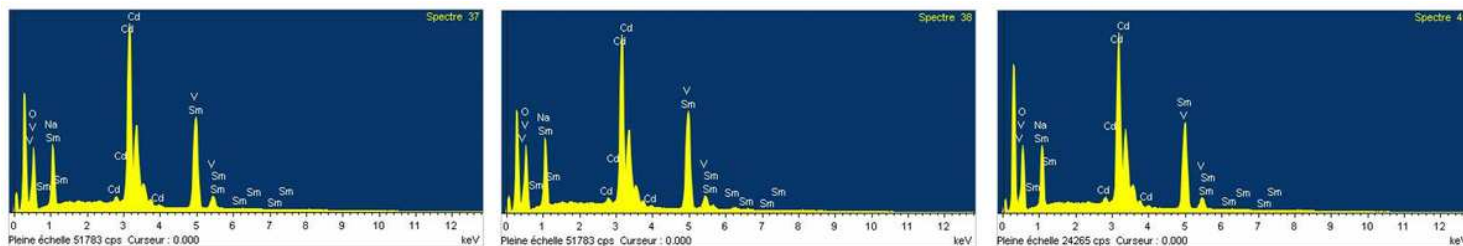


Figure 2

EDS spectra of NaCdVO₄:xSm compounds

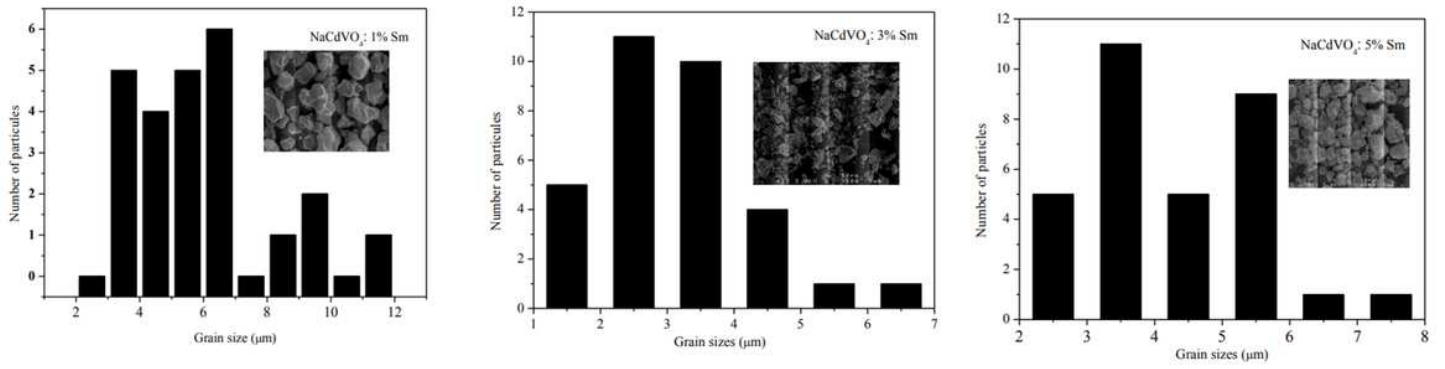


Figure 3

Size distribution histograms of NaCdVO₄:xSm phosphors

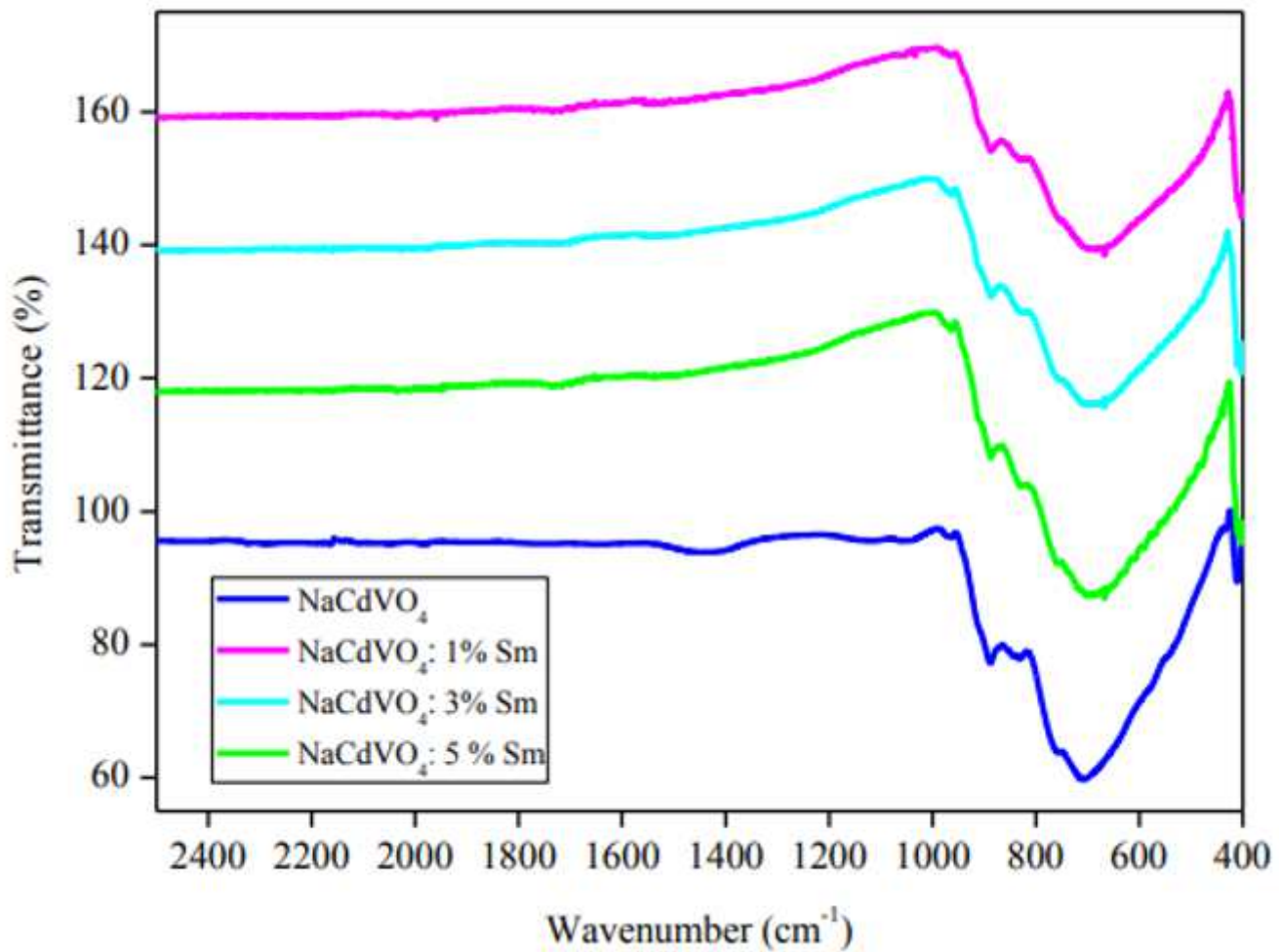


Figure 4

IR spectra of NaCdVO₄:xSm phosphors

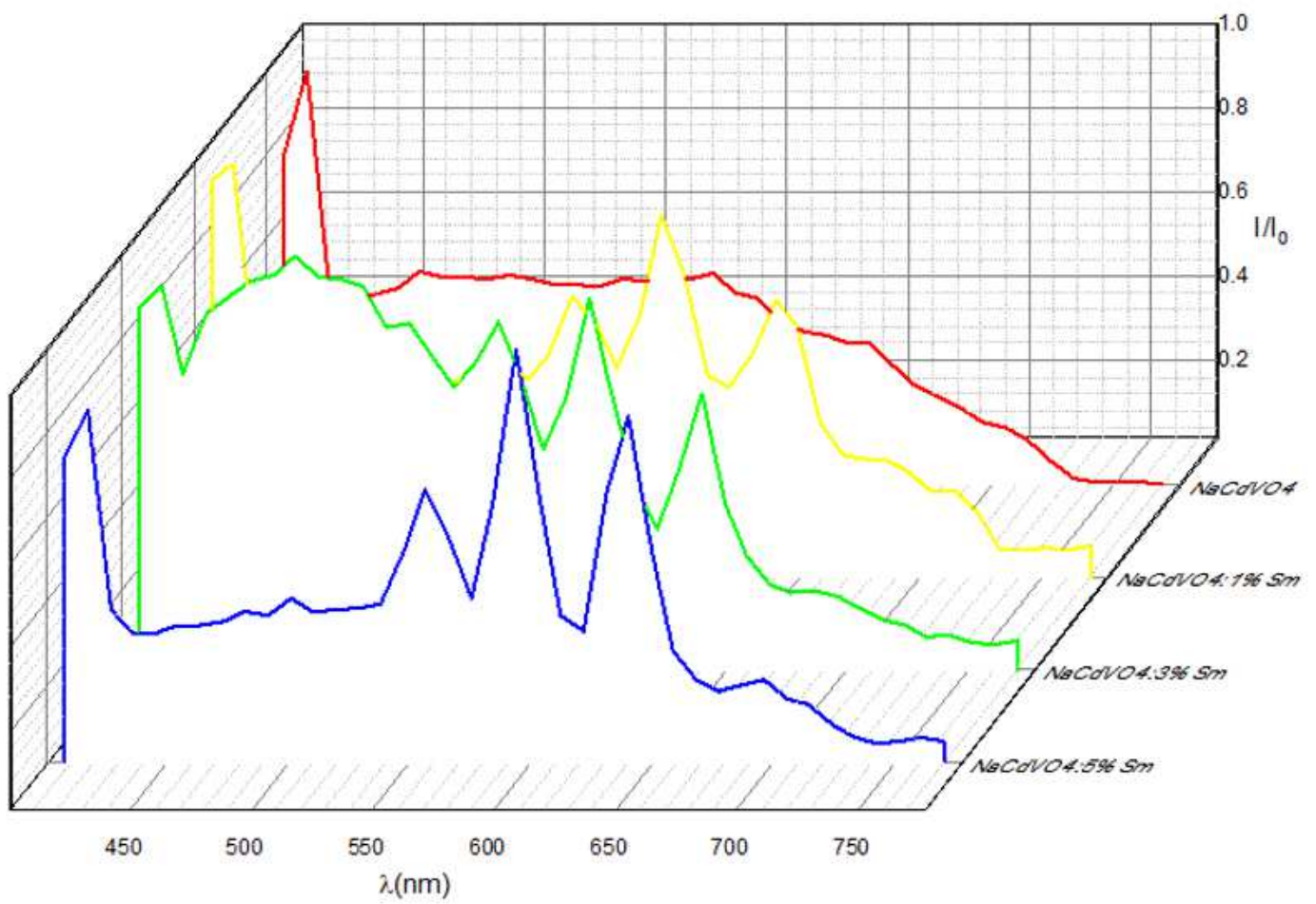


Figure 5

Room-temperature PL emission spectra of the as a function of wavelength under 405nm excitation

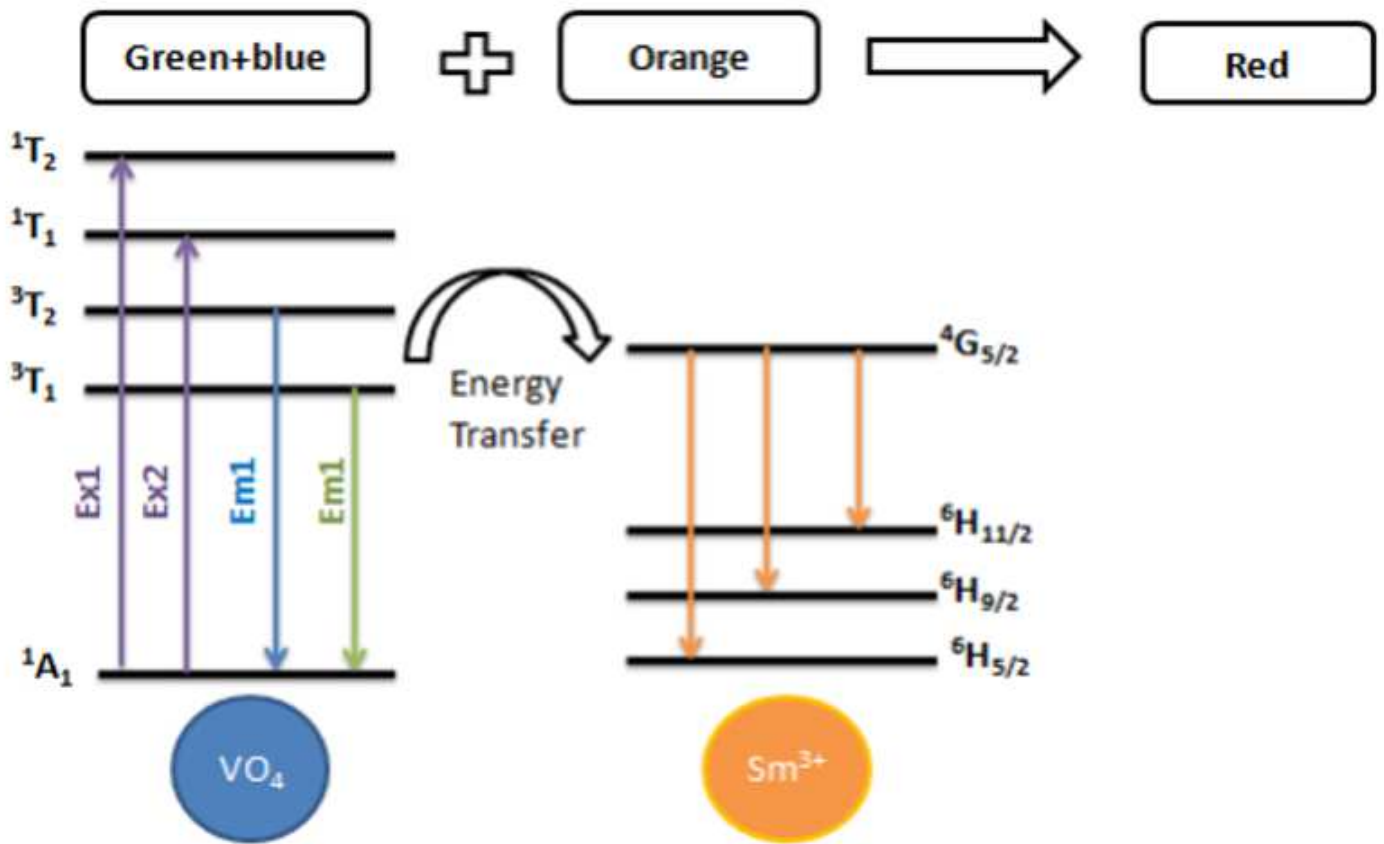


Figure 6

Schematic of the energy transfer process from $[\text{VO}_4]^{3-}$ to Sm^{3+} in $\text{NaCdVO}_4:\text{xSm}$ phosphors

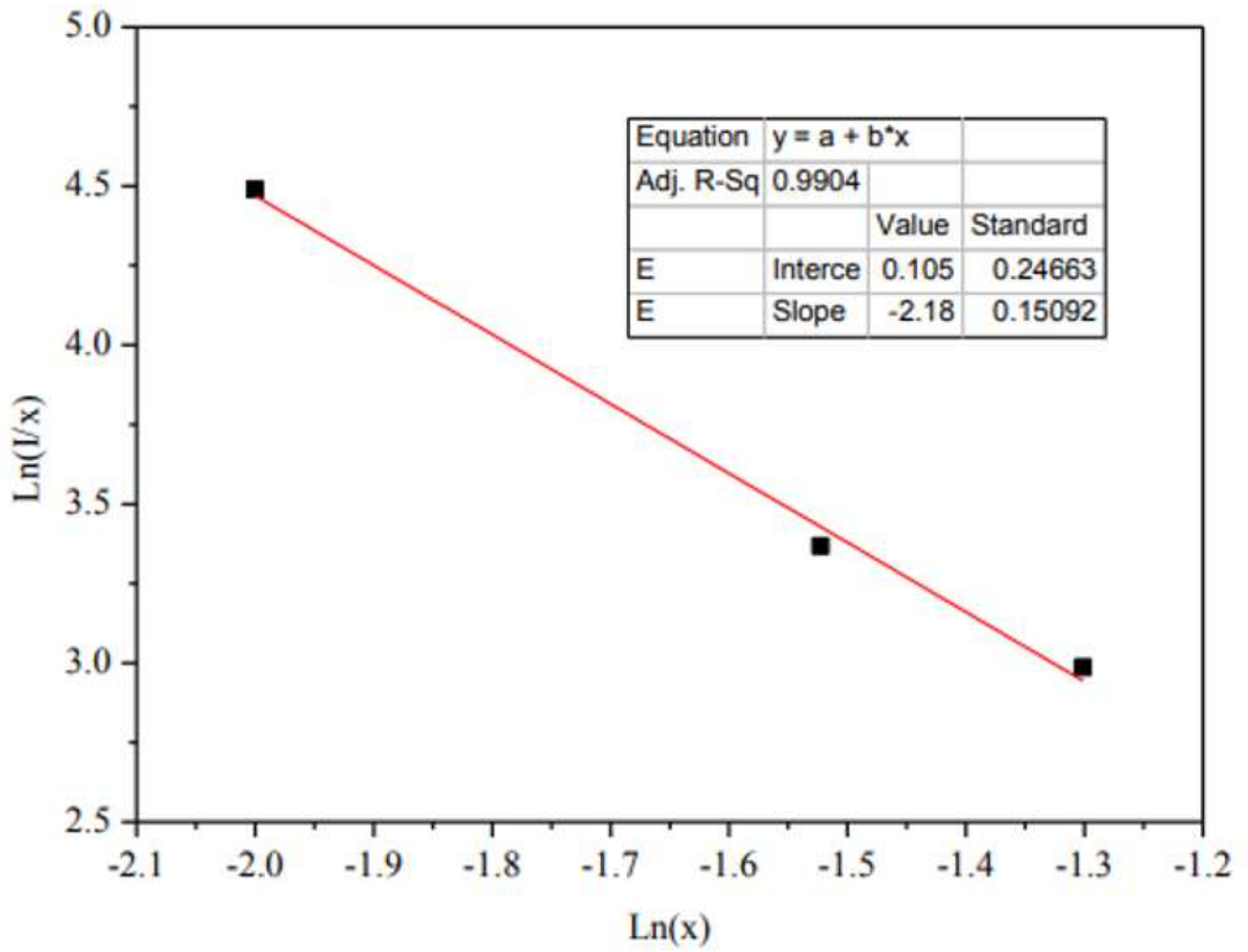


Figure 7

Plot of $\log(I/x)$ versus $\log(x)$ for the $4G_{5/2} \rightarrow 6H_{7/2}$ transition of Sm^{3+} ions in $NaCdVO_4: xSm$ phosphors

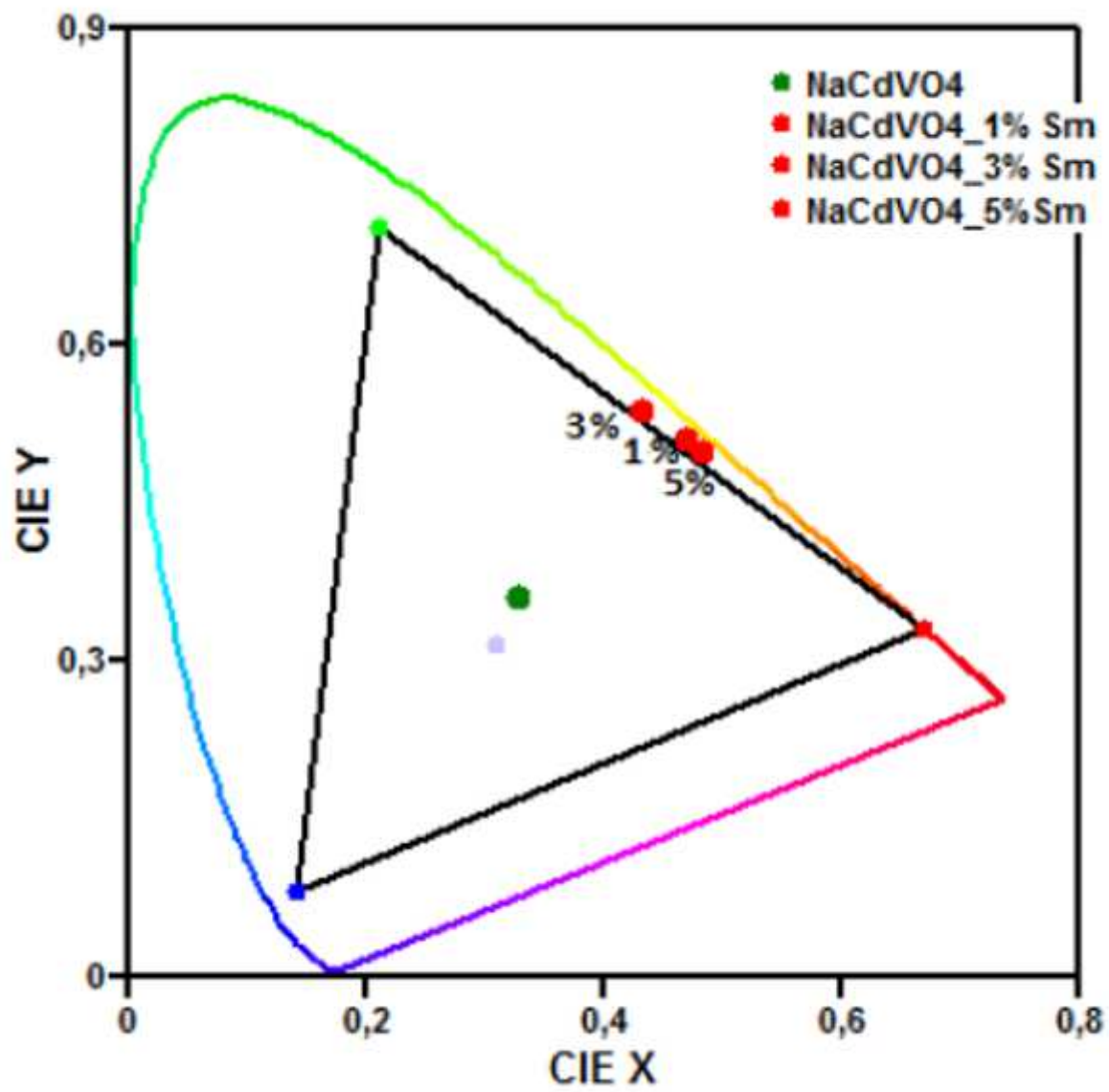


Figure 8

CIE chromaticity coordinates of NaCdVO₄ doped with Sm³⁺

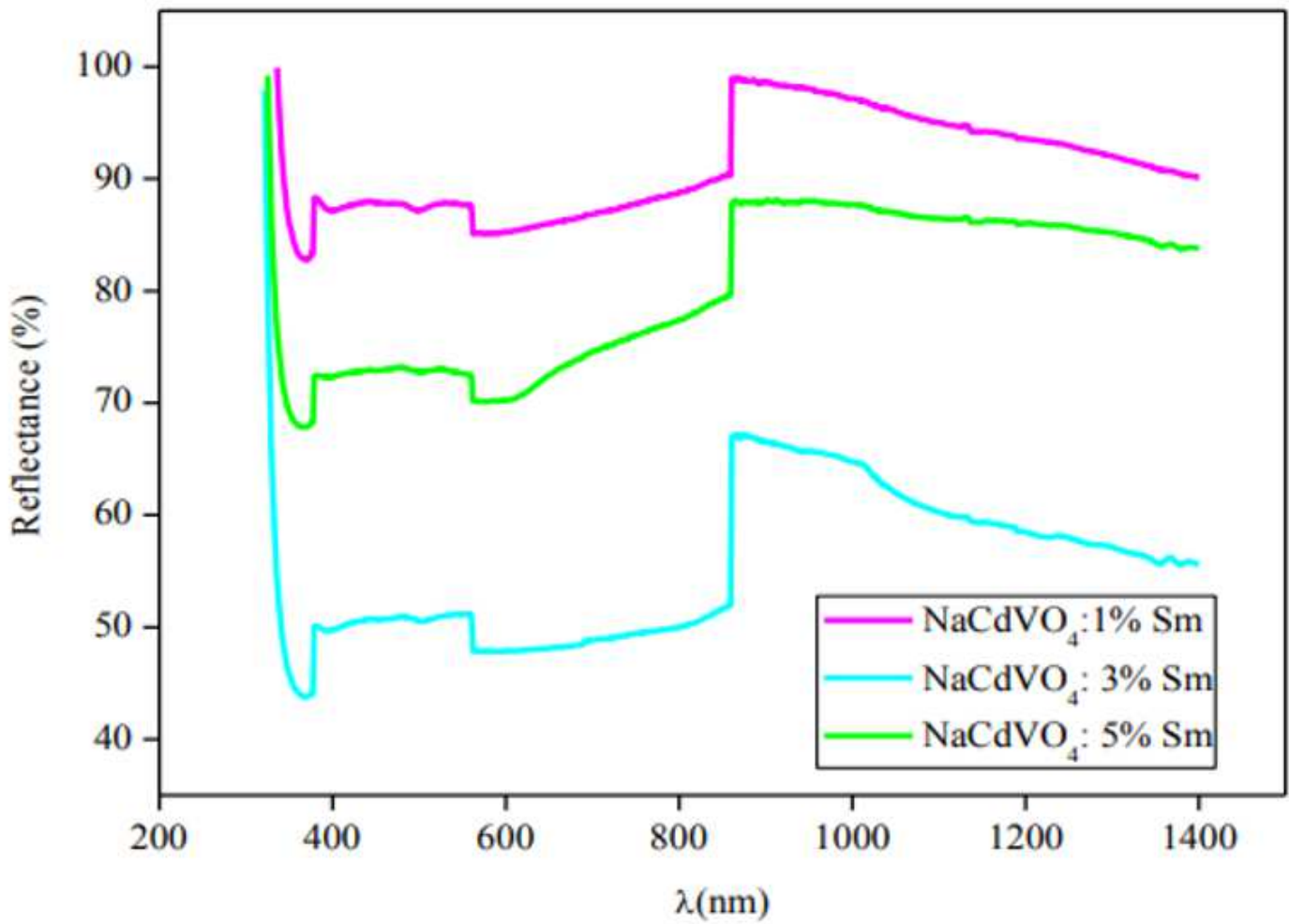


Figure 9

Reflectance spectra of NaCdVO₄:xSm phosphors

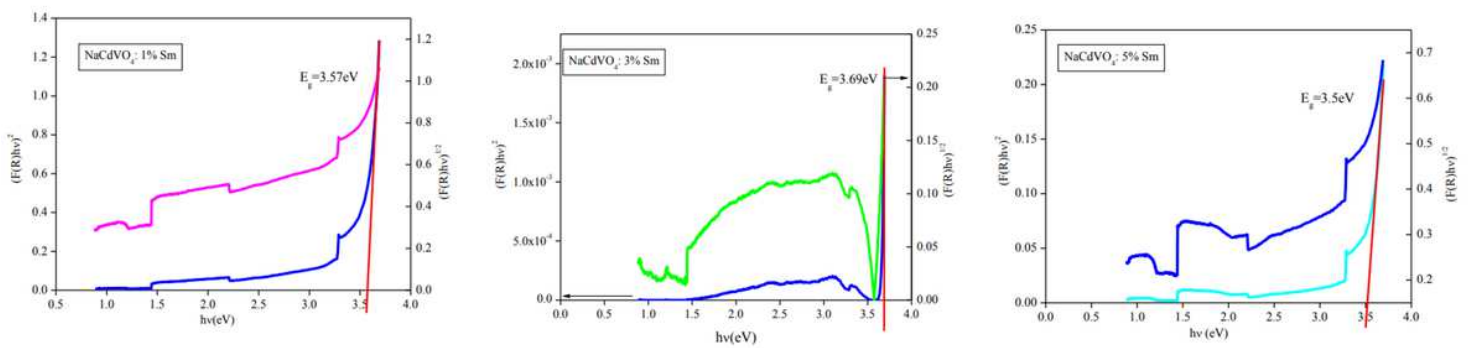


Figure 10

Plots of $(ah\nu)^{1/2}$ and $(ah\nu)^2$ versus $(h\nu)$ of NaCdVO₄:xSm phosphors